Large impact of strain on the electro-optic effect in (Ba, Sr)TiO$_3$ thin films: Experiment and theoretical comparison ⓕ

Shinya Kondo, Tomoaki Yamada ⓘD, Alexander K. Tagantsev, Ping Ma ⓘD, Juerg Leuthold ⓘD, Paolo Martelli, Pierpaolo Boffi, Mario Martinelli, Masahito Yoshino, and Takanori Nagasaki

COLLECTIONS

Ⓕ This paper was selected as Featured

View Online Export Citation CrossMark

ARTICLES YOU MAY BE INTERESTED IN

Domain structure formation by electron beam irradiation in lithium niobate crystals at elevated temperatures
Applied Physics Letters 115, 092903 (2019); https://doi.org/10.1063/1.5108962

Influence of the polarization anisotropy on the linewidth enhancement factor and reflection sensitivity of 1.55-μm InP-based InAs quantum dash lasers
Applied Physics Letters 115, 091101 (2019); https://doi.org/10.1063/1.5110768

Ferroelectric domain structures and temperature-misfit strain phase diagrams of $K_{1-x}Na_xNbO_3$ thin films: A phase-field study
Applied Physics Letters 115, 092902 (2019); https://doi.org/10.1063/1.5116910

Large impact of strain on the electro-optic effect in (Ba, Sr)TiO$_3$ thin films: Experiment and theoretical comparison

View Online   Export Citation   CrossMark

Shinya Kondo,[1] Tomoaki Yamada,[1,a)] Alexander K. Tagantsev,[2,3] Ping Ma,[4] Juerg Leuthold,[4] Paolo Martelli,[5] Pierpaolo Boffi,[5] Mario Martinelli,[5] Masahito Yoshino,[1] and Takanori Nagasaki[1]

AFFILIATIONS

[1]Department of Energy Engineering, Nagoya University, Furo-cho, Chikusa-ku, Nagoya 464-8603, Japan
[2]Ioffe Physical-Technical Institute, 26 Politekhnicheskaya, Saint Petersburg 194021, Russia
[3]Institute of Materials Science, Swiss Federal Institute of Technology (EPFL), Lausanne CH-1015, Switzerland
[4]Institute of Electromagnetic Fields, ETH Zurich, Zurich CH-8092, Switzerland
[5]Department of Electronics, Information and Bioengineering, Politecnico di Milano, Milano 20133, Italy

a)E-mail: t-yamada@energy.nagoya-u.ac.jp

ABSTRACT

(001)-epitaxial (Ba$_{0.5}$Sr$_{0.5}$)TiO$_3$ (BST) thin films with different magnitudes of compressive strain were fabricated on SrRuO$_3$/SrTiO$_3$ substrates by pulsed laser deposition, and their electro-optic (EO) properties were characterized by modulation ellipsometry at different temperatures. All fabricated films showed an increased paraelectric-to-ferroelectric phase transition temperature upon compressive strain and revealed c-domain structures in the ferroelectric phase. We experimentally clarified that the EO properties of compressively strained BST thin films are enhanced toward the phase transition temperature modified by the strain. The experimental results were compared with the theoretical prediction based on a phenomenological thermodynamic model. Although the measured EO coefficient r_c was less than that theoretically predicted, the experimentally observed strain effect on the EO properties is in good qualitative agreement.

Published under license by AIP Publishing. https://doi.org/10.1063/1.5117218

In recent years, novel thin-film-based electro-optic (EO) modulators, which are compact, energy-saving, and high-speed, have attracted a great deal of attention.[1–3] In such devices, the use of ferroelectric materials, which show large EO coefficients, such as BaTiO$_3$ (BTO),[3–5] is preferable compared to that of nonlinear polymers from the points of view of long-term stability.[1,2] However, it is widely observed that the EO coefficients of thin ferroelectric films are often different from those of the bulks.[4–7] Although there are several possible factors influencing the EO properties of ferroelectric thin films, such as the fabrication process and microstructure,[4] the most influential factor would be the strain on the films since these dielectric properties are known to be significantly strain-sensitive.[8–11] Fredrickson et al., Hamze et al., and Paillard et al. recently reported on the theoretical prediction of the effects of such strain on BTO, SrTiO$_3$ (STO), and PbTiO$_3$ thin films using first-principles calculations, respectively, in which they predicted that the EO properties can be enhanced by the softening of the soft mode phonon via strain engineering.[12–14]

However, the experimental proof of this concept has not yet been clearly demonstrated.

In this study, we experimentally demonstrate the effect of compressive strain on the EO properties of (001)-epitaxial (Ba$_{0.5}$Sr$_{0.5}$)TiO$_3$ (BST) thin films and show that the EO properties of BST thin films are enhanced toward the phase transition temperature modified by the strain. We also demonstrate that the phenomenological thermodynamic model reasonably supports our experimental results.

The results are presented in the following manner: first, the phenomenological model of the EO properties is derived for the compressively strained (001)-epitaxial BST thin films. Then, structural and electrical characterization studies of the films on SrRuO$_3$ (SRO)/STO substrates grown by pulsed laser deposition (PLD) are presented. The EO properties of the fabricated BST films are measured by modulation ellipsometry, constructed for thin films. The temperature dependence of the EO property of the BST films with different strains is investigated and compared with the phenomenological thermodynamic model.

To estimate the strain effect on the EO properties of BST thin films theoretically, we use a phenomenological thermodynamic theory, which can be reasonably applied to ferroelectric materials, including solid solution systems like the BST examined in this study. The phenomenological thermodynamic models of the EO properties of ferroelectric films were initially reported by Qiu et al., Liu et al., and Chen et al.[15–18] We recently expanded the models, taking into account not only the intrinsic EO effects but also the elasto-optic effects, from the converse piezoelectric response of the films.[19] The inverse permittivity at optical frequencies of a ferroelectric thin film, which has spontaneous polarization, can be written as[20,21]

$$\varepsilon_{ij}(0)^{-1} = \delta_{ij}\varepsilon_{C}^{-1} + g_{ijkl}^{S}P_{S,k}P_{S,l} + p_{ijkl}^{P}u_{0,kl}, \qquad (1)$$

to which the dummy suffix summation rule is applied. Here δ_{ij}, ε_{C}, g_{ijkl}^{S}, and p_{ijkl}^{P} are the Kronecker delta ($\delta_{ij} = 1$ for $i = j$ and $\delta_{ij} = 0$ for $i \neq j$), the permittivity of the cubic state, the quadratic polarization-optic tensor at constant strain, and the elasto-optic tensor at constant polarization, respectively. $P_{S,i}$ is the spontaneous polarization, and $u_{0,kl}$ is the lattice deformation caused by spontaneous polarization and mismatch with the substrate. When an electric field, E_m, is applied to the film, the inverse permittivity is modified to become

$$\varepsilon_{ij}^{-1}(E_m) = \varepsilon_{ij}^{-1}(0) + \left(2g_{ijkl}^{S}P_{S,k}\chi_{lm} + p_{ijkl}^{P}d_{mkl}^{f}\right)E_m, \qquad (2)$$

where χ_{lm} and d_{mkl}^{f} are the electric susceptibility at low frequencies and the piezoelectric coefficient of the film, respectively. The parentheses in Eq. (2) correspond to the linear EO coefficient r_{ijm}, in which the first term describes the intrinsic EO effect and the second term describes the elasto-optic effect arising from the converse piezoelectric response.

In the case of (001)-epitaxial BST thin films, it has been theoretically and experimentally clarified that the ferroelectric, tetragonal c-domain phase is induced by compressive strain on cooling from the paraelectric cubic phase.[9,22–24] Therefore, in the present theory, we only focus on the paraelectric and ferroelectric c-domain phases, where ε_{ij} is diagonal. We should also note that the electric field E_3 was applied parallel to the spontaneous polarization $P_{S,3}$; thus, E_3 does not affect the diagonality of ε_{ij}. Namely, no rotation of the optical indicatrix is caused by E_3. Applying this condition into the films, we find

$$r_{113} = 2g_{1133}^{S}P_{S,3}\chi_{33} + p_{1133}^{P}d_{333}^{f}, \qquad (3)$$

$$r_{333} = 2g_{3333}^{S}P_{S,3}\chi_{33} + p_{3333}^{P}d_{333}^{f}, \qquad (4)$$

$$d_{333}^{f} = d_{333} - 2\left(s_{1122}/(s_{1111} + s_{1122})\right)d_{311}. \qquad (5)$$

As in Eq. (5), d_{333}^{f} in the film is written using d_{333} and d_{311} and the elastic compliances s_{1111} and s_{1122}.[25] Therefore, the numerical estimation of r_{113} and r_{333} requires the temperature- and strain-dependent parameters $P_{S,3}$, χ_{33}, and d_{333}^{f}, which can be calculated using the modified thermodynamic potential.[22,23,26,27] Since r_{113} and r_{333} cannot be separately measured in the experiment, we calculated "measurable" effective EO coefficient $r_c = r_{333} - (n_1/n_3)^3 r_{113}$, arising from the change in the difference between the two principal refractive indexes $n_1 (= \sqrt{\varepsilon_{11}(0)})$ and $n_3 (= \sqrt{\varepsilon_{33}(0)})$, for comparison with our experiment.[28]

Figure 1 shows the estimated temperature–strain map for the effective EO coefficient, r_c, of a $(Ba_{0.5}Sr_{0.5})TiO_3$ film. As can be clearly

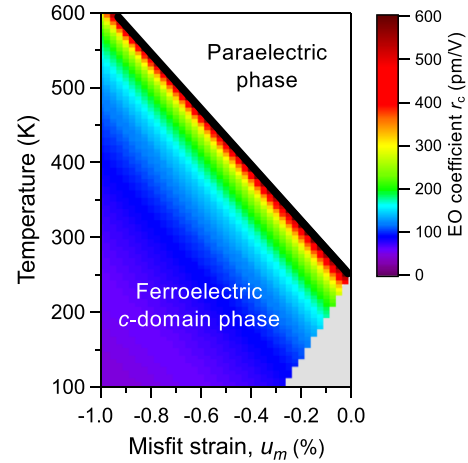FIG. 1. Effective EO coefficient, r_c, estimated for a c-domain $(Ba_{0.5}Sr_{0.5})TiO_3$ thin film as a function of temperature and misfit strain.

seen, the largest EO response is expected near the paraelectric-to-ferroelectric phase transition temperature modified by the strain, a tendency of which also agrees with recent reports using first-principles calculations.[12–14] In addition, it is worth mentioning that the magnitude of the EO response is mainly determined by the difference in temperature from the paraelectric-to-ferroelectric phase transition boundary.

To demonstrate the theoretically predicted behavior experimentally, BST thin films with different film thicknesses, from 50 to 300 nm, were fabricated at 700 °C in 10 mTorr O_2 on SRO/STO (001) substrates by PLD with a KrF excimer laser ($\lambda = 248$ nm). SRO bottom electrodes of thickness 20 nm were also fabricated by PLD at 700 °C in 200 mTorr O_2. The laser energy was 60 mJ, and the repetition rates were 7 and 10 Hz for the BST and SRO films, respectively. A ceramic pellet of $(Ba_{0.5}Sr_{0.5})TiO_3$ prepared using a standard sintering process and a commercially available SRO ceramic pellet were used as targets for the PLD. After depositing the BST films, circular platinum layers of diameter 100 or 200 μm and thickness 10 nm were deposited by electron beam evaporation as semi-transparent top electrodes. The crystal structure, orientation, crystallinity, and strain of the fabricated BST films were characterized by X-ray diffraction (XRD) using a four-axis diffractometer with Cu–$K_{\alpha 1}$ X-rays. A precision LCR meter was used to investigate the dielectric properties of the BST films.

All the fabricated films showed the full width at half maximum of the rocking curve for 002 reflection $\leq 0.1°$, indicating the high crystallinity of the films. Figure 2(a) shows the XRD reciprocal space map around BST 203 for the films with different thicknesses measured at room temperature. In the case of 50 nm thickness, the in-plane lattice constant of the BST film was almost the same as that of the STO substrate, indicating that the film was almost fully constrained by the substrate. With the increasing thickness, the peak position of the BST gradually shifted to the line of the cubic lattice due to the strain relaxation. Finally, that of the 300-nm-thick BST film almost approached the cubic line, indicating that the phase transition temperature is close to room temperature; thus, the film behaves more like bulk materials, for which the transition temperature is 250 K. It is also noted that all fabricated films have a c-domain structure at room temperature,
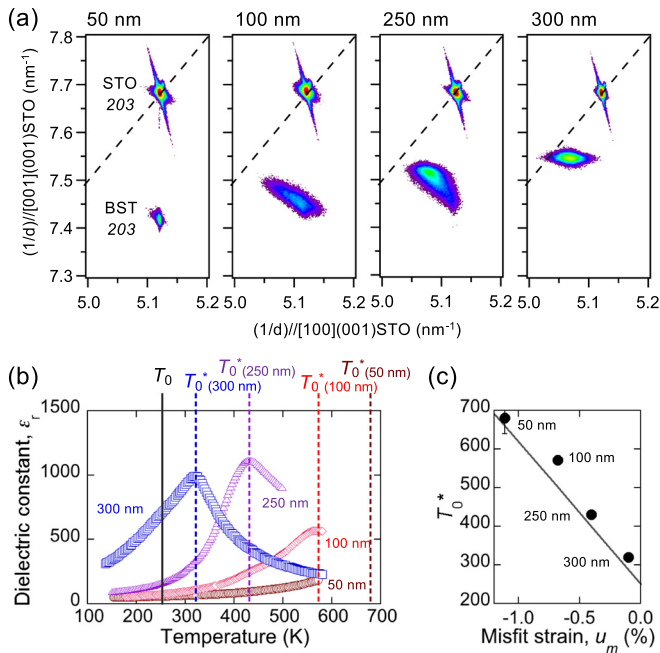
FIG. 2. (a) XRD reciprocal space maps at room temperature around BST 203 for BST thin films on SRO/STO substrates with different film thicknesses: 50, 100, 250, and 300 nm. The dashed lines correspond to the cubic lattices. (b) Temperature dependence of the dielectric constant, ε_r, for the BST films measured at 1 kHz. The paraelectric-to-ferroelectric phase transition temperature for bulk, $T_0 (= 250\,K)$, and that for the films, T_0^*, are shown using solid and dashed lines, respectively. (c) Strain dependence of T_0^* of the films. The solid line is for the theoretical prediction.

TABLE I. In-plane and out-of-plane lattice parameters, misfit strain u_m, and phase transition temperature, T_0^*, for the BST films with different thicknesses.

Film thickness (nm)	In-plane lattice parameter (Å)	Out-of-plane lattice parameter (Å)	u_m (%)	T_0^* (K)
50	3.906	4.044	-1.11 ± 0.03	680 ± 40
100	3.923	4.020	-0.68 ± 0.03	571 ± 10
250	3.934	3.992	-0.41 ± 0.03	430 ± 10
300	3.946	3.975	-0.10 ± 0.03	320 ± 10

To investigate the EO properties of the BST thin films with different magnitudes of strain, modulation ellipsometry was performed.[4,5,30–32] The schematic diagram of the experimental set-up is shown in Fig. 3(a). A polarized He–Ne laser ($\lambda = 632.8\,nm$) was transmitted through the samples mounted on a heater with an incident angle of $\theta = 45°$ and a polarization angle of $\phi = 45°$ to efficiently reveal the modulation intensity from the c-domain BST films. A sinusoidal voltage of 0.3 V peak-to-peak amplitude at 1 kHz, with a DC voltage, is applied to the samples using a function generator. This alternate voltage causes a linear EO phase modulation, hence a variable birefringence of the sample, transforming a laser beam with stable linear polarization at the sample input into a beam with modulated elliptic polarization at the sample output. A quarter-wave plate after the samples compensates for the ellipticity of the polarization, in order to maximize the modulation depth after the analyzer, which converts the EO phase modulation into an amplitude modulation of the optical beam. The modulation amplitude was detected by a photodetector followed by a lock-in amplifier.
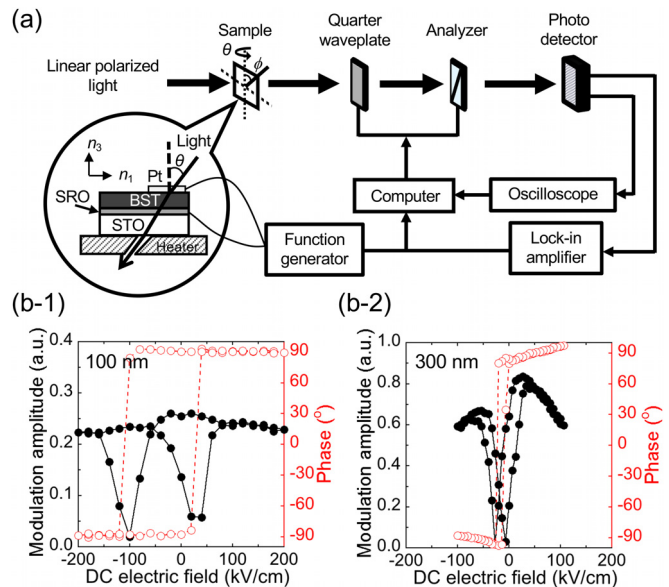
meaning that the films can have either a single domain or 180° domains without an electric field applied.

Figure 2(b) shows the temperature dependence of the dielectric constant for the films with different thicknesses measured at 1 kHz. Except for the 50-nm-thick film, the paraelectric-to-ferroelectric phase transition temperature of the films, T_0^*, was defined from the peaking temperature of the dielectric constant, as indicated by the dashed lines. On the other hand, T_0^* for the 50-nm-thick film was estimated from the temperature dependence of the lattice constant measured by XRD (not shown here) because of the out of examined temperature range for the dielectric measurement. The transition temperature of the unstrained bulks $T_0 (= 250\,K)$ is also indicated by a solid line in the figure.[29] In compressively strained (001) BST thin films, T_0^* is theoretically expected to be increased by the strain as

$$T_0^* = T_0 + 4\varepsilon_0 C \frac{Q_{1122}}{s_{1111} + s_{1122}} u_m, \qquad (6)$$

where ε_0, C, Q_{1122}, and u_m are the vacuum permittivity, the Curie–Weiss constant, the electrostrictive coefficient, and the in-plane misfit strain of BST films, respectively.[26] Indeed, all fabricated films showed T_0^* higher than T_0, and T_0^* monotonically increased with the decreasing film thickness, namely, with the increasing compressive strain, which is in good agreement with the theoretical prediction as shown in Fig. 2(c).[22–24] The lattice constants and strain, as well as the phase transition temperature of the fabricated BST films, are summarized in Table I.

FIG. 3. (a) Schematic of the ellipsometric EO measurement set-up. (b) DC electric field dependence of the modulation amplitude for the 100-nm-thick BST (b-1) and 300-nm-thick BST (b-2) films at room temperature.

Figures 3(b-1) and 3(b-2) show the dependence of the modulation amplitude on the DC electric field at room temperature for the 100- and 300-nm-thick BST films, respectively, as typical examples. It was found that the phase was changed by 180° by sweeping the DC electric field, which clearly showed the polarization reversal of the BST films regardless of the thickness. Nevertheless, it should be mentioned that, unlike the films with a thickness of 250 nm and below, the 300-nm-thick BST film showed the large humps in the modulation amplitude hysteresis as can be seen in Fig. 3(b-2). Such a hysteresis shape is also known for a piezoelectric response, where the field-induced effect and domain reorientation contribution interplay.[33,34] For the 300-nm-thick BST film at room temperature, the field-induced effect cannot be neglected as T_0^* is close to room temperature. In addition, a wider hysteresis was observed for the thinner film because of the higher ferroelectric-to-paraelectric phase transition temperature owing to the larger compressive strain (see Table I) and the additional thin film effect that a coercive field is larger for a thinner film.

On the basis of the approximation $n_1 \approx n_3$, r_c was estimated from the measured modulation amplitude as has been reported in literature studies.[30–32,35] Figure 4(a) shows the temperature dependence of the effective EO coefficient, r_c, for the BST films with different magnitudes of strain. For this measurement, the DC electric field in a range of 30–50 kV/cm was applied to the 50-, 100-, and 250-nm thick films in order to avoid the 180° polarization switching by the alternate voltage and thus to ensure the single domain state. The DC electric field was also applied to the 300-nm thick film to be consistent with the others although the field-induced effect cannot be neglected as described above. It should also be mentioned that the provided theoretical model is for the EO response without a DC field. Nevertheless, it is comparable to the experiment at least for the films with a thickness of 250 nm and below, in which the ferroelectric-to-paraelectric phase transition temperature is far above the examined temperatures.

For the thinner 50- and 100-nm-thick films, which have large compressive strains ($u_m = -1.11\%$ and -0.68%), r_c remained almost constant or showed a slight increase with respect to temperature. For the 250-nm-thick film, which has a weaker compressive strain ($u_m = -0.41\%$), showed larger r_c and a strong increase with temperature. On the other hand, for the 300-nm-thick film, the strain of which is largely relaxed ($u_m = -0.10\%$), r_c decreased with temperature.
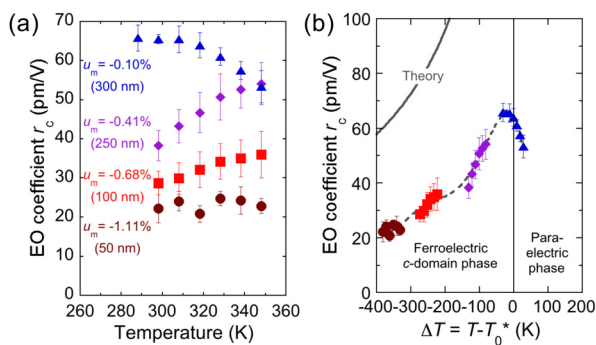
These results can be better summarized from the point of view of the difference in temperature from the paraelectric-to-ferroelectric phase transition temperature, i.e., $\Delta T = T - T_0^*$. Figure 4(b) shows the dependence of r_c on ΔT for all films. As can be clearly seen, r_c increased with temperature toward the phase transition temperature, T_0^*, which is in good agreement with the fundamental feature of the theoretical prediction described above.

In contrast, r_c decreased but did not disappear above T_0^* although the linear EO response should be absent in the paraelectric phase in the given theoretical model. This can be mainly due to the smeared phase transition of the fabricated films, which might be attributed to small but nonnegligible strain distribution. The remanence of certain polarity above T_0^* would result in the detectable linear EO response in the films. In addition, the quadratic EO response may also be appreciable as the electric field induced polarization becomes larger. The comprehensive systematic study is required to clarify the EO response above T_0^* in the future.

One should also notice that the experimentally measured r_c was always less than that theoretically predicted. The main reason for this difference would be the long-range electrostatic contribution to the size-effect, the so-called dead layer effect.[36] This effect has been commonly observed in the ferroelectric films with parallel plate electrodes and has been widely discussed that the field seen by the ferroelectric films is smaller than that applied to the films as the ferroelectric/electrode interface behaves as a thin layer with a low dielectric constant. Indeed, the EO coefficients reported for BST films with coplanar electrodes, for which the dead layer effect can be neglected, are larger than those observed in the present study.[7,37] For instance, the experimentally observed and theoretically predicted values of the dielectric constant at around 290 K for the 300 nm-thick film were 868 and 1767, respectively, the ratio of which is around 1:2. Therefore, for this specific condition, the field seen by the ferroelectric can be about half of that applied to the film; thus, the observed EO coefficient will also be reduced to half, which can reasonably explain the difference in the magnitude of r_c between the experiment and the theory. Note that the magnitude of the dead layer effect can be affected by both the film thickness and the strain; the former varies the capacitance of the ferroelectric layer, and the latter varies the dielectric constant of the ferroelectric layer and hence also the capacitance. Therefore, the magnitude of the dead layer effect should be different for different films. Nevertheless, the field seen by the ferroelectric in our films at the temperatures for the EO measurement was estimated to be within the range of 0.5–0.8 of that applied to the films, which does not change the basic trend of the temperature dependence of the EO coefficient. Therefore, the observed temperature dependence clearly demonstrates the fundamental feature of the enhancement of the EO response at the phase transition temperature modified by the strain.

In summary, we first modeled the linear EO effects for compressively strained (001)-epitaxial BST thin films, which have a c-domain structure in the ferroelectric phase, based on phenomenological thermodynamic theory. Then, the BST films, which have different magnitudes of compressive strain, were fabricated on SRO/STO substrates. The effective EO coefficients of the fabricated BST films were measured by modulation ellipsometry and were compared with the theory. It was experimentally clarified that the EO responses of compressively strained (001)-epitaxial BST thin films increased with temperature toward the paraelectric-to-ferroelectric phase transition temperature

FIG. 4. (a) Temperature dependence of the effective EO coefficient, r_c, measured for the BST thin films with different magnitudes of misfit strain on SRO/STO substrates. (b) r_c as a function of the difference in temperature from phase transition temperature, $\Delta T = T - T_0^*$. Theoretical values are indicated using solid lines.

modified by the strain. The observed behavior was in good qualitative agreement with the theoretical prediction. Our experimental findings suggest that the strain engineering of ferroelectric thin films is a powerful tool for manipulating not only their dielectric, piezoelectric, and ferroelectric properties but also their EO properties.

REFERENCES

[1] A. Melikyan, L. Alloatti, A. Muslija, D. Hillerkuss, P. C. Schindler, J. Li, R. Palmer, D. Korn, S. Muehlbrandt, D. Van Thourhout, B. Chen, R. Dinu, M. Sommer, C. Koos, M. Kohl, W. Freude, and J. Leuthold, Nat. Photonics **8**, 229 (2014).

[2] A. Messner, F. Eltes, P. Ma, S. Abel, B. Baeuerle, A. Josten, W. Heni, D. Caimi, J. Fompeyrine, and J. Leuthold, J. Lightwave Technol. **37**, 281 (2019).

[3] S. Abel, F. Eltes, J. E. Ortmann, A. Messner, P. Castera, T. Wagner, D. Urbonas, A. Rosa, A. M. Gutierrez, D. Tulli, P. Ma, B. Baeuerle, A. Josten, W. Heni, D. Caimi, L. Czornomaz, A. A. Demkov, J. Leuthold, P. Sanchis, and J. Fompeyrine, Nat. Mater. **18**, 42 (2019).

[4] K. J. Kormondy, Y. Popoff, M. Sousa, F. Eltes, D. Caimi, M. D. Rossell, M. Fiebig, P. Hoffmann, C. Marchiori, M. Reinke, M. Trassin, A. A. Demkov, J. Fompeyrine, and S. Abel, Nanotechnology **28**, 075706 (2017).

[5] S. Abel, T. Stöferle, C. Marchiori, C. Rossel, M. D. Rossell, R. Erni, D. Caimi, M. Sousa, A. Chelnokov, B. J. Offrein, and J. Fompeyrine, Nat. Commun. **4**, 1671 (2013).

[6] H. Ma, J. Levy, M. D. Biegalski, S. Trolier-McKinstry, Darrell, and G. Schlom, J. Appl. Phys. **105**, 014102 (2009).

[7] D. Y. Wang, J. Wang, H. L. W. Chan, and C. L. Choy, J. Appl. Phys. **101**, 043515 (2007).

[8] J. H. Haeni, P. Irvin, W. Chang, R. Uecker, P. Reiche, Y. L. Li, S. Choudhury, W. Tian, M. E. Hawley, B. Craigo, A. K. Tagantsev, X. Q. Pan, S. K. Streiffer, L. Q. Chen, S. W. Kirchoefer, J. Levy, and D. G. Schlom, Nature **430**, 758 (2004).

[9] C. L. Canedy, H. Li, S. P. Alpay, L. Salamanca-Riba, A. L. Roytburd, and R. Ramesh, Appl. Phys. Lett. **77**, 1695 (2000).

[10] H. Li, A. L. Roytburd, S. P. Alpay, T. D. Tran, L. Salamanca-Riba, and R. Ramesh, Appl. Phys. Lett. **78**, 2354 (2001).

[11] T. Yamada, K. F. Astafiev, V. O. Sherman, A. K. Tagantsev, P. Muralt, and N. Setter, Appl. Phys. Lett. **86**, 142904 (2005).

[12] K. D. Fredrickson, V. V. Vogler-Neuling, K. J. Kormondy, D. Caimi, F. Eltes, M. Sousa, J. Fompeyrine, S. Abel, and A. A. Demkov, Phys. Rev. B **98**, 075136 (2018).

[13] A. K. Hamze and A. A. Demkov, Phys. Rev. Mater. **2**, 115202 (2018).

[14] C. Paillard, S. Prokhorenko, and L. Bellaiche, npj Comput. Mater. Sci. **5**, 6 (2019).

[15] J. H. Qiu, J. N. Ding, N. Y. Yuan, X. Q. Wang, and Y. Zhou, Solid State Commun. **151**, 1344 (2011).

[16] J. H. Qiu and Q. Jiang, J. Appl. Phys. **102**, 074101 (2007).

[17] P. F. Liu and Q. Jiang, Phys. Lett. A **352**, 451 (2006).

[18] L. Chen, Y. Zhang, Q. Guo, D. Zhang, X. Zhong, and J. Yuan, Appl. Phys. Lett. **105**, 112903 (2014).

[19] S. Kondo, T. Yamada, A. Tagantsev, N. Setter, M. Yoshino, and T. Nagasaki, J. Ceram. Soc. Jpn. **127**, 348 (2019).

[20] S. H. Wemple and M. DiDomenico, Jr., J. Appl. Phys. **40**, 735 (1969).

[21] P. Bernaconi, M. Zgonik, and P. Günter, J. Appl. Phys. **78**, 2651 (1995).

[22] Z.-G. Ban and S. P. Alpay, J. Appl. Phys. **91**, 9288 (2002).

[23] Z.-G. Ban and S. P. Alpay, J. Appl. Phys. **93**, 504 (2003).

[24] T. Yamada, T. Kamo, H. Funakubo, D. Su, and T. Iijima, J. Appl. Phys. **109**, 091605 (2011).

[25] K. Lefki and G. J. M. Dormans, J. Appl. Phys. **76**, 1764 (1994).

[26] N. A. Pertstev, A. G. Zembilgotov, and A. K. Tagantsev, Phys. Rev. Lett. **80**, 1988 (1998).

[27] All of the coefficients used in the thermodynamic calculation for BST are listed in Ref. 19.

[28] I. P. Kaminow and E. H. Turner, Appl. Opt. **5**, 1612 (1966).

[29] A. D. Hilton and B. W. Ricketts, J. Phys. D: Appl. Phys. **29**, 1321 (1996).

[30] S. H. Han and J. W. Wu, J. Opt. Soc. Am. B **14**, 1131 (1997).

[31] Y. Levy, M. Dumont, E. Chastaing, P. Robin, P.-A. Chollet, G. Gadret, and F. Kajzar, Mol. Cryst. Liq. Cryst. Sci. Technol., Sect. B **4**, 1 (1993).

[32] C. B. Ma, D. Xu, Q. Ren, Z. H. Lv, H. L. Yang, F. Q. Meng, G. H. Zhang, S. Y. Guo, L. X. Sang, and Z. G. Wang, J. Mater. Sci. Lett. **22**, 49 (2003).

[33] A. K. Tagantsev, P. Muralt, and J. Fousek, Mater. Res. Soc. Symp. Proc. **784**, C10.6 (2003).

[34] D.-Y. Chen and J. D. Phillips, J. Electroceram. **17**, 613 (2006).

[35] The refractive indices of BST films should change with temperature and misfit strain. However, in this evaluation, we regard n as 2.2 from Ref. 7 since the effect of the change in n on EO coefficients is negligible.

[36] A. K. Tagantsev, Size Effects in Ferroelectric-Containing Structures, Encyclopedia of Materials: Science and Technology, 2nd ed. (Elsevier, Amsterdam, 2011).

[37] J. Li, F. Duewer, C. Gao, H. Chang, X.-D. Xiang, and Y. Lu, Appl. Phys. Lett. **76**, 769 (2000).